

A high-resolution Ramsey-Bordé spectrometer for optical clocks based on cold Mg atoms

J. Keupp, A. Douillet, T.E. Mehlstäubler, N. Rehbein, E.M. Rasel^a, and W. Ertmer

Institute for Quantum Optics, University of Hannover, Welfengarten 1, 30167 Hannover, Germany

Received 30 May 2005 / Received in final form 1st August 2005

Published online 16 November 2005 – © EDP Sciences, Società Italiana di Fisica, Springer-Verlag 2005

Abstract. We report on recent progress in our Ramsey-Bordé interferometer with cold magnesium atoms at 457.2 nm. A resolution as high as $\Delta\nu = 290$ Hz was achieved, which corresponds to a quality factor of $Q = 2.3 \times 10^{12}$. An upper limit of 170 Hz for the laser oscillator line width is inferred from the interferometric analysis of the contrast decay induced by the residual atomic motion and spontaneous emission. The performance of the spectrometer allows to realize an optical frequency standard at 457.2 nm with a short-term stability of up to $\sigma_y(\tau = 1\text{ s}) = 8 \times 10^{-14}$ with 10^5 atoms similar to state-of-the art, non-cryogenic microwave clocks or oscillators.

PACS. 06.30.Ft time and frequency – 39.20.+q atom interferometry techniques – 39.25.+k Atom manipulation (scanning probe microscopy, laser cooling, etc.)

1 Introduction

Recent progress in atomic cooling and trapping [1–7] as well as in frequency division by comb generators [8,9] turned optical frequency standards based on ions and atoms into promising candidates for new primary standards. Ultimately, they are expected to combine an excellent short-term stability and an accuracy which is comparable or better than state-of-the-art microwave clocks [10,11]. In comparison to single-ion clocks, the main advantage of neutral atom clocks is their higher short-term stability due to simultaneous spectroscopy of typically 10^6 atoms. The development of appropriate cooling and trapping techniques is still an issue with respect to the achievable accuracy. We report on the progress and prospects for a future frequency standard based on magnesium. Key-elements of optical clocks and frequency standards are a stable oscillator and an atomic reference with a high quality factor. In this respect, magnesium is an excellent candidate as it offers ultra-narrow transitions such as the intercombination lines $^1S_0 \rightarrow ^3P_{0,1,2}$ at $\lambda = 457.2$ nm with linewidths of 31 Hz and less. With our Ramsey-Bordé interferometer probing the $3^1S_0 \rightarrow 3^3P_1(m=0)$ transition, a resolution of 290 Hz was achieved. Major improvements were made in terms of frequency stability of our dye laser system and in a better signal-to-noise ratio due to a stable number of trapped atoms. We have investigated the individual contributions to the observed signal decay at long interrogation times. At temperatures close to the Doppler limit, $T_{Dopp} = 2$ mK, the effect of the residual motion of the atoms is still significant. Its influence on the signal was analyzed in detail by interferometric meth-

ods combined with Monte-Carlo simulations of the atomic ensemble.

The experimental results underline the need for efficient cooling techniques in order to increase the resolution of our interferometer. Extracting the effect of atomic motion on the contrast decay, an upper limit for the linewidth of the dye laser of 170 Hz is deduced. When improving the resolution of the interferometer and the temperature of the atomic ensemble by using more advanced cooling techniques, the frequency noise of the laser becomes even more important for the performance of the frequency standard [12].

Dye lasers exhibit a broad intrinsic noise spectrum, which extends up to several megahertz. Nevertheless sub-Hertz linewidths have been achieved [13]. For magnesium, a solid-state laser system based on Nd:YVO₄ appears to be a promising alternative. We have demonstrated the coincidence of the second harmonic of the $^4F_{3/2} \rightarrow ^4I_{9/2}$ transition in Nd:YVO₄ with our clock transition.

2 Experimental set-up

Our experimental studies were performed with a Ramsey-Bordé type interferometer based on laser cooled magnesium atoms, similar as described in [14]. Here, we briefly summarize the main parts and point out major changes and improvements.

An iodine-stabilized rhodamine dye laser combined with a second harmonic generation in a BBO crystal provides 70 mW of light at 285.2 nm for cooling and trapping ^{24}Mg on the closed $3^1S_0 \rightarrow 3^1P_1$ transition. MOT and interferometer are alternately operated with a cycling rate of 48 s^{-1} . The fluorescence of the trapped

^a e-mail: rasel@iqo.uni-hannover.de

atoms is averaged over 1 s. After the interferometry cycle only atoms in the ground state are recaptured by the MOT. The Ramsey-Bordé interferometer modulates the recapture rate by exciting a fraction of the atoms to the long-lived state 3^3P_1 with a life time of 5.1 ms. These atoms have a high probability to escape from the capture range of the MOT before they decay to the ground state. Hence, the stationary number of trapped atoms defined as equilibrium between loading from a thermal beam and atomic escape, reflects the population in the ground state at the exit ports of the interferometer [15,16]. For our setup, the highest stability in the number of trapped atoms was achieved for an average number of 10^5 atoms. The temperature of the ensemble was typically 3.8 mK, well above the theoretical Doppler limit ($T_{Dopp} = 2$ mK).

The UV light for the MOT is transported over a 5 m distance with an active beam pointing stabilization system. In order to suppress power fluctuations and cross coupling of power and pointing instabilities we have implemented a two step power stabilization based on acousto-optical modulators (AOM) with an estimated servo bandwidth of a few tens of kilohertz. Thus, we are able to reduce fluctuations in the number of trapped atoms to less than 0.6% for 1 second observation time.

The spectroscopy laser at $\lambda = 457.2$ nm is based on a stilbene dye laser with an output power of 120 mW. The first frequency stabilization stage consists of a Pound-Drever-Hall (PDH) type servo lock [17] onto a stable Zerodur optical resonator. It controls a fast intra-cavity electro-optical modulator and a piezo-operated mirror of the laser resonator. The feedback loop is designed for a modulation frequency of 13.5 MHz and a unity-gain bandwidth of 2 MHz. This scheme reduces the laser linewidth to 870 Hz measured with a second resonator made of ultra-low-expansion material (ULE) and with Ramsey-Bordé contrast interferometry [14]. The residual frequency instability is mainly caused by mechanical vibrations of the optical table, on which the Zerodur cavity is rigidly mounted.

To improve the linewidth we stabilize, in addition, our laser system on the ULE resonator with a finesse of $\mathfrak{F} = 39.000$. For efficient suppression of mechanical vibrations, the resonator is equipped with a three-stage vibration isolation system. Inside its vacuum chamber, the resonator is suspended by a two-stage spring-pendulum damped by Eddy-currents. The system is mounted on a granite plate (150 kg) attached by rubber ropes (1.8 m) to the laboratory ceiling. This massive pendulum has a resonance frequency of 2.9 Hz and the residual acceleration on the granite plate is measured to be below 8×10^{-7} g (rms) at a resolution bandwidth of 0.24 Hz. According to the Young's modulus of ULE, this upper limit of the mechanical noise should lead to a linewidth well below 150 Hz. An optical fiber, guiding the light to the granite platform, provides stable coupling of the laser light into the resonator.

The ULE resonator shows a remarkably slow drift of the average frequency. The two years average is 0.03 Hz s^{-1} and the maximum drift observed over minutes is $\pm 3 \text{ Hz s}^{-1}$ as seen in Figure 1. The drift rates

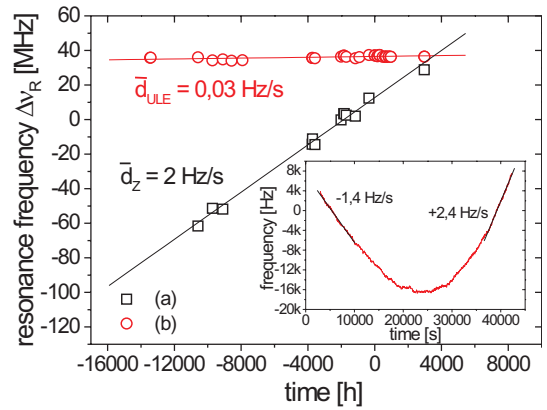


Fig. 1. Drift of the Zerodur (a) and ULE (b) resonator over 2 years with respect to our magnesium beam reference. The insert shows a typical short term drift behavior of the ULE cavity.

are measured with respect to our Ramsey-Bordé atomic beam interferometer. The second PDH stabilization onto the ULE resonator operates at a modulation frequency of 9.7 MHz. Frequency excursions up to 20 kHz are compensated for by steering the frequency of the double-passed AOM which shifts the laser onto resonance with the first cavity. The residual long-term drift is corrected by stabilizing the laser to a magnesium atom beam interferometer. With this two-stage scheme, the dye laser's linewidth is finally reduced to 170 Hz. This value is an upper limit and was deduced by measuring the contrast decay of the time-domain Ramsey-Bordé interferometer for increasing resolutions.

The temporal sequence of the atomic beam-splitting pulses is generated by two AOMs. The light pulses are focused to a waist of $w_0 = 3.4$ mm at the center of the MOT. For an atomic temperature of 3.8 mK, the beam waist limits the interaction time to about 2 ms. For longer interaction times, the atoms leave the interferometer zone. The magnetic field of the MOT is switched off $150 \mu\text{s}$ before the first interferometer pulse. The chosen pulse length of $4 \mu\text{s}$ is a compromise between the optimal beam splitting ratio ($\tau_{\pi/2} = 6 \mu\text{s}$) and a broad Fourier bandwidth, which excites about 9% of the atomic velocity distribution. The frequency resolution of the interferometer is adjusted by varying the dark time T between the first and the second as well as between the third and the fourth laser pulse. To ensure that the fringe patterns of the two interferometers originating from the two possible directions of the photon recoil overlap constructively, the resolution has to be chosen such that the recoil shift δ_r is an integral multiple of the resolution. In magnesium, this shift is $\delta_r = h/(2M\lambda^2)$ giving $\delta_r = 39.62$ kHz.

3 Spectroscopic results

The potential short-term stability of our optical interferometer was characterized with the Ramsey-Bordé interferometer.

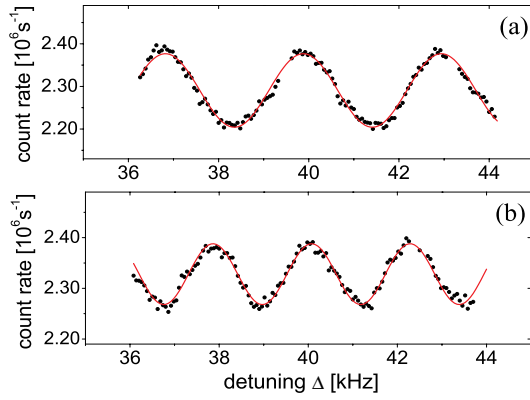


Fig. 2. Frequency sensitive low noise interference fringes at moderate resolution of $\Delta\nu = 1530$ Hz (a) and 1105 Hz (b).

We investigated the various contributions that can deteriorate the interference signal: residual laser instability, atomic motion and frequency/phase perturbations during the transport of the light to the atoms.

We evaluate the potential stability of the laser frequency locked to this interference signal in terms of the Allan standard deviation, which in our case can be estimated according to

$$\sigma_y(\tau) = \frac{1}{\pi Q S/N} \sqrt{\frac{t_m}{\tau}} \quad (1)$$

for an integration time τ , as given in [18]. The standard deviation is derived from the signal to noise ratio (S/N) and the quality factor $Q = \nu_0/\Delta\nu$. For the S/N , S is the half-wave amplitude of the interference signal and N the noise — i.e. the observed variance σ — of the photon count rate. Offsets due to detector dark counts or stray light were at negligible level. The resolution $\Delta\nu$ is defined as the FWHM of the frequency dependent sinusoidal interference pattern. It is determined by the time of free evolution T according to $\Delta\nu = 1/(4T)$. t_m is the averaging time for one data point. The dominant noise process is assumed to be white noise. In this work, the Allan variance is deduced from the interferometric measurement for 1 s integration time. For short time scales, the assumption of white noise is applicable. For longer times we observe systematic drifts due to fluctuations of the number of trapped atoms (our measurement scheme does not include an atom number normalization). Figure 2 shows the interference signals with the highest signal to noise ratio at resolutions of $\Delta\nu = 1530$ Hz and $\Delta\nu = 1105$ Hz. The averaging time for one data point is $t_m = 1.05$ s corresponding to 50 interferometry cycles. We fit a sinusoidal with a period according to the applied pulse sequence. The signal to noise ratio is calculated using the standard deviation of the difference between the data points and the fitted function. The achieved S/N of 8.4 and 6.2 leads to a stability of $\sigma_y(1\text{ s}) = 8.9 \times 10^{-14}$ and $\sigma_y(1\text{ s}) = 8.7 \times 10^{-14}$, respectively. We increase the resolution up to $\Delta\nu = 290$ Hz with a time of free evolution of $T = 860.8 \mu\text{s}$ as shown in Figure 3.

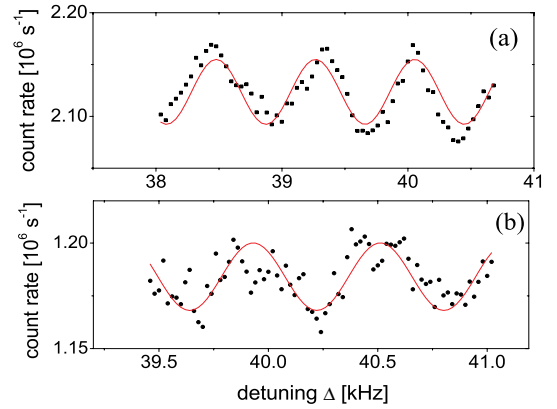


Fig. 3. High resolution and high stability interference signals with $\Delta\nu = 394$ Hz (a) and 290 Hz (b).

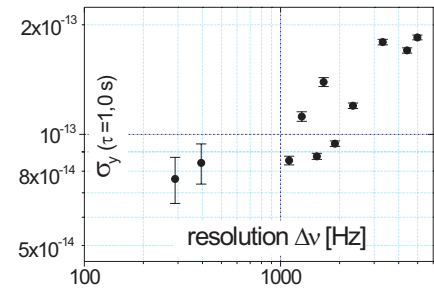


Fig. 4. Potential stability as a function of the resolution of the interferometer signal. The best value of $\sigma_y(1\text{ s}) = 8 \times 10^{-14}$ is obtained with the highest resolution. Error bars in this figure display the quality of individual measurements. Dye laser and atom trap performance, however, appear as a scatter in the calculated stability values for different measurement days.

The maximum observed stability was $\sigma_y(1\text{ s}) = 7.8 \times 10^{-14}$ with a quality factor $Q = 2.26 \times 10^{12}$ similar to state-of-the-art non-cryogenic microwave clocks [10]. Today's best microwave clock based on cryogenic sapphire oscillators [19] achieve a stability of $\sigma_y(1\text{ s}) = 1.6 \times 10^{-14}$ [11].

Figure 4 summarizes the deduced stability as a function of the resolution. The Allan variance is clearly reduced for increasing resolutions and finally saturates near $\sigma_y(1\text{ s}) = 8 \times 10^{-14}$ at $\Delta\nu = 1$ kHz. Below 1 kHz, the decreasing signal amplitude balances the effect of the increase in resolution. At higher resolutions, the signal to noise ratio is reduced to 1.8 as the atoms start to leave the interrogation zone. The amplitude diminishes also due to phase fluctuations of the spectroscopy laser and due to frequency perturbations of the light on the way to the atoms. In order to deduce an upper limit for the laser linewidth, we investigated this effect with our atom interferometer and extracted this contribution using a numerical model.

We operate the Ramsey-Bordé interferometer with moderate resolution of $\Delta\nu = 4.4$ kHz. In this case, the atomic motion is negligible during the short duration of the interferometer sequence (0.115 ms). We analyze the decrease of the interference signal at different expansion times of the atomic cloud, by varying the time when the

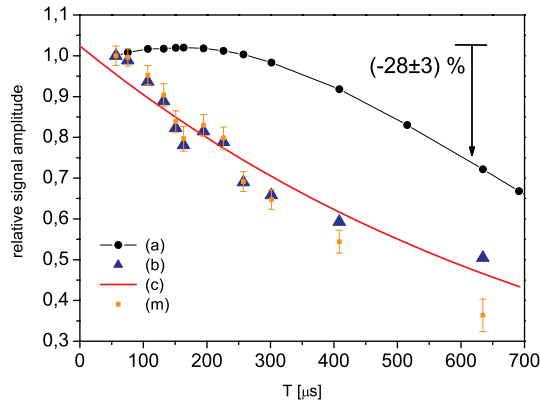


Fig. 5. The observed amplitude decay (m) of the interference pattern with increasing dark time T . The contribution of the atomic motion as well as the spontaneous emission is calculated with a Monte-Carlo simulation (a). The exponential fit (c) of the residual amplitude decay (b) serves as a rough measure for the laser linewidth (170 Hz). The analysis is only based on the amplitude of the interference pattern (AC part) and does not include the background or DC contribution.

pulse sequence starts. The measurement reveals that the highest signal amplitude was obtained with the interferometer placed slightly above the MOT center. This indicates that the atomic ensemble is released with a center of mass motion directed upwards. For increasing delays of the start of the pulse sequence (up to 500 μs), the better overlap between the atomic cloud and the beam splitting laser leads to a higher signal amplitude of the interference pattern. For longer delays, the amplitude decreases due to the isotropic expansion of the atomic cloud. We compare the characteristic variation of the signal with a Monte-Carlo simulation and extract the Gaussian sigma σ_v of the velocity distribution, the center of mass velocity v_{cms} perpendicular to the Ramsey-Bordé interferometer beams and a spatial offset y_L of the MOT position to the center of the interaction zone. For a specific adjustment of the MOT we find $\sigma_v = (1.4 \pm 0.4)$ m/s, $v_{cms} = (1.2 \pm 0.1)$ m/s and $y_L = (1850 \pm 50)$ μm . The Monte-Carlo simulation averages the de-Broglie wave amplitudes in the ground or excited state for the specific paths of up to 10^5 atoms. We include the decay due to spontaneous emission.

An accuracy of 5% is estimated from parameter variations within the experimental error bars. Figure 5 shows the variation of the measured signal amplitude (m) with increasing interrogation time T . The model predicts the amplitude decay (a) due to atomic motion and spontaneous emission. For $T = 634.6$ μs the amplitude reduction amounts to $(-28 \pm 3)\%$. The residual atomic motion alone leads to a decrease of 19% in the relative signal amplitude.

After correcting the measured amplitudes with the simulation results, one obtains the decay function due to the phase fluctuations of the light at the location of the atom interferometer. An exponential fit allows to quantify the laser stability in terms of an equivalent linewidth for white frequency noise. We determine a spectral width of $\delta\nu \leq (170 \pm 15)$ Hz. The spectral width of the op-

tical field measured with this method provides only an upper boundary. Another contribution to the observed linewidth is related to the light transport. The light from the laser oscillator is transported between two laser tables over about 5 m distance with an active beam pointing stabilization. Evaluating the phase fluctuations accumulated on this path by a heterodyne measurement we observe a contribution of 20 Hz up to 100 Hz to the linewidth. Measurements also indicate that an additional intensity stabilization of our dye laser will improve the performance of our laser spectrometer. Intensity variations on one hand lead to an AM-FM noise conversion in the Pound-Drever-Hall lock and, on the other hand, they degrade the actively controlled beam pointing. In order to reduce these effects we have implemented a power stabilization with an AOM operated in 0th order. Adjusting the radio frequency power by the servo leads to strong beam pointing fluctuations which we attribute to the varying heat flow within the AOM crystal. Instead, we operate the AOM at constant RF power, and change the diffraction efficiency by adjusting the frequency. This technique drastically reduces the beam pointing fluctuations. A full evaluation of the influence of the improved power stability has still to be completed. At a resolution of $\Delta\nu = 1283$ Hz (1530 Hz) we observe a gain in the interferometer signal amplitude by 30% (10%). The amplitude gain, depending on the realized resolution, clearly indicates a reduction of phase fluctuations.

4 Further development

The presented measurements underline the importance of the precise control of the atomic motion for the performance of our Ramsey-Bordé interferometer. A reduction of the atomic temperature makes it possible to increase the interrogation times as well as to lower systematic errors [21]. For colder atoms, the spectral width of the Doppler profile and of the excitation pulse can be perfectly matched, which increases the signal to noise ratio. In the present experiment, only a minor fraction of 9% of the trapped atoms is excited. For alkaline-earth atoms, several strategies may provide an avenue to μK temperatures [1–7]. We investigate the cooling of magnesium on ultra-narrow transitions. This cooling technique was successfully implemented for calcium by several groups [1–3] and is expected to be appropriate for magnesium. In magnesium we identified the transition $3^3\text{P}_1 \rightarrow 4^1\text{S}_0$ as most favourable candidate for the quenching process [22]. The expected final temperature in a MOT configuration, operating on quenched transitions (Quench-MOT) is about 10 μK , i.e. more than two orders of magnitude lower than the Doppler limit for the singlet transition. The effects of the residual atomic motion, as observed in this work, will be substantially reduced. For 4 μs Ramsey pulses, nearly the full Doppler profile (more than 70%) of the atomic ensemble will contribute to the interference signal, resulting in a high contrast. The higher excitation efficiency will eventually compensate for the substantial loss of fast atoms during the transfer into the Quench-MOT. Based

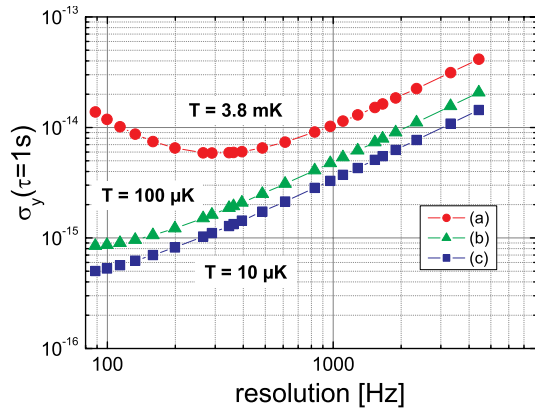


Fig. 6. Estimation of the possible stability of an oscillator locked to a Ramsey-Bordé spectrometer based on ultra-cold atoms (c). The minimum instability will be $\sigma_y(1\text{ s}) = 7 \times 10^{-16}$ with 10^5 atoms. For comparison ultimate values for cold atoms at 3.8 mK (a) and 100 μK (b) are shown.

on the Monte-Carlo simulation described above, with an estimate of 10^5 ultra-cold atoms, one can expect a stability of $\sigma_y(1\text{ s}) = 7 \times 10^{-16}$ at a resolution of $\Delta\nu = 100\text{ Hz}$ as to be seen in Figure 6.

The expected stability should exceed the possible values for ion clocks significantly. For single Hg^+ ions the quantum projection noise limit will be reached at about $\sigma_y(1\text{ s}) = 2 \times 10^{-15}$ [23]. The simulation does not include the Dick effect, which describes the influence of the noise of the spectroscopy laser on the frequency stability [24–26]. Ultimately, the achievable frequency stability depends on the spectral noise of the spectroscopy laser and the sensitivity function of the interferometer, which is determined by the resolution, and the duration of the atomic preparation and detection. Generally, a large duty cycle, $d = 2T/T_c$, defined as the ratio of the interferometry sequence and the full measurement cycle (including preparation as well as detection of the atoms) reduces the effect of the spectral noise of the spectroscopy laser on the instability [28]. Simulations show that quench cooling extends the atomic preparation by about 20 to 30 ms, which is still less than the time of at least 100 ms for loading the MOT with 10^6 atoms. For a typical resolution of 200 Hz (2.5 ms duration of the full interferometer sequence), the atomic preparation results in a duty cycle larger than 0.03. To obtain a short-term stability of 10^{-15} in 1 s as anticipated in Figure 6, a laser frequency noise level of about $100\text{ mHz}/\sqrt{\text{Hz}}$ at frequencies above $f_c = 1/T_c$ is required [28]. The Dick effect, hence, sets severe demands on the spectroscopy laser. We therefore plan to replace the currently used dye laser with its high intrinsic frequency noise by a frequency-doubled Nd:YVO₄ solid-state laser, with a thin-disc geometry [27]. The laser system, based on a semifocal cavity with two etalons, provides about 1 Watt at 914 nm in the TEM₀₀ mode and is pumped with two 20 W diode lasers. The second harmonic of the transition $^4\text{F}_{3/2} \rightarrow ^4\text{I}_{9/2}$ in Nd:YVO₄ covers the spectrum of the intercombination transitions in magnesium. The coincidence with the clock transition was demonstrated by

a heterodyne measurement of our dye laser system locked to a thermal magnesium beam and the second harmonic generated in single pass in PPKTP. In the future, comparisons of the laser line widths are possible by direct beating of the dye laser and solid state laser light fields. Another possible all-solid-state solution for the interferometry laser could involve a diode laser and tapered amplifier as source for the fundamental wavelength of 914 nm.

5 Conclusion and outlook

Summarizing our work, this paper reports on our current activities to develop an optical frequency standard for magnesium. We demonstrated a Ramsey-Bordé interferometer with resolutions as high as 290 Hz at 655 THz — one of the key elements of an atomic frequency standard. The performance of this set-up permits to stabilize the frequency of a laser with a short term stability of up to $\sigma_y(1\text{ s}) = 8 \times 10^{-14}$. Major improvements are a two-stage frequency lock on an ultra-stable resonator and a very reproducible preparation of the atoms. The residual thermal and center of mass motion of the atoms is shown to be a major limit for further improvement of resolution and stability. The precise preparation of atoms at low temperature is also crucial for the achievable accuracy. We have pointed out possible strategies to achieve ultra-cold temperatures and intrinsically stable lasers for magnesium. With these techniques a stability of $\sigma_y(1\text{ s}) = 10^{-15}$ should be in reach. Heading towards this regime, laser sources exhibiting frequency noise levels below $1\text{ Hz}/\sqrt{\text{Hz}}$ at relevant frequencies have recently been demonstrated, using a rather simple and robust new mounting scheme for the reference cavity [29]. A major task is the precise measurement of the clock transition frequency for magnesium and a detailed study of systematic errors. Nowadays, optical comb generators and lasers at 914 nm provide a practical solution. With all these ingredients, we believe magnesium to represent an interesting candidate for future frequency standards and frequency comparisons, which are of high relevance for fundamental tests such as the verification of constancy of basic physical constants.

References

1. T. Binnewies, G. Wilpers, U. Sterr, F. Riehle, J. Helmcke, T.E. Mehlstäubler, E.M. Rasel, W. Ertmer, Phys. Rev. Lett. **87**, 123002 (2001)
2. E.A. Curtis, C.W. Oates, L. Hollberg, Phys. Rev. A **64**, 031403 (2001)
3. E.A. Curtis, C.W. Oates, L. Hollberg, J. Opt. Soc. Am. B **20**, 977 (2003)
4. M. Takamoto, F.-L. Hong, R. Higashi, H. Katori, Nature **435**, 321 (2005)
5. Y. Takasu, K. Maki, K. Komori, T. Takano, K. Honda, M. Kumakura, T. Yabuzaki, Y. Takahashi, Phys. Rev. Lett. **91**, 0404041 (2003)
6. X. Xu, T.H. Loftus, J.L. Hall, A. Gallagher, J. Ye, J. Opt. Soc. Am. B **20**, 968 (2003)
7. J. Grünert, A. Hemmerich, Phys. Rev. A **65**, 041401 (2002)

8. Th. Udem, J. Reichert, T.W. Hänsch, *Opt. Lett.* **24**, 881 (1999)
9. D.J. Jones, S.A. Diddams, J.K. Ranka, A. Stenz, R.S. Windeler, J.L. Hall, S.T. Cundiff, *Science* **288**, 635 (2000)
10. S. Weyers, U. Hübner, R. Schröder, C. Tamm, A. Bauch, *Metrologia* **38**, 343 (2001)
11. C. Vian, P. Rosenbusch, H. Marion, S. Bize, L. Cacciapuotti, S. Zhang, M. Abgall, D. Chambon, I. Maksimovic, P. Laurent, G. Santarelli, A. Clairon, A. Luiten, M. Tobar, C. Salomon, *IEEE Trans. Instrum. Meas.* **54**, 2 (2005)
12. U. Sterr, C. Degenhardt, H. Stoehr, Ch. Lisdat, H. Schnatz, J. Helmcke, F. Riehle, G. Wilpers, Ch. Oates, L. Hollberg, *C. R. Phys.* **5**, 845 (2004)
13. B.C. Young, F.C. Cruz, W.M. Itano, J.C. Bergquist, *Phys. Rev. Lett.* **82**, 3799 (1999)
14. F. Ruschewitz, J.L. Peng, H. Hinderthür, N. Schaffrath, K. Sengstock, W. Ertmer, *Phys. Rev. Lett.* **80**, 3173 (1998)
15. W. Nagourney, J. Sandberg, H. Dehmelt, *Phys. Rev. Lett.* **56**, 2797 (1986)
16. K. Sengstock, U. Sterr, G. Hennig, D. Bettermann, J.H. Müller, W. Ertmer, *Opt. Comm.* **103**, 73 (1993)
17. R.W.P. Drever, J.L. Hall, F.V. Kowalski, J. Hough, G.M. Ford, A.J. Munley, H. Ward, *App. Phys. B* **31**, 97 (1983)
18. F. Riehle, *Frequency Standards - Basics and Applications* (Weinheim, Wiley-VCH, 2004)
19. A.G. Mann, C. Sheng, A.N. Luiten, *IEEE Trans. Instrum. Meas.* **50**, 519 (2001)
20. S. Bize, P. Laurent, M. Abgrall, H. Marion, I. Maksimovic, L. Cacciapuotti, J. Grünert, C. Vian, F. Pereira dos Santos, P. Rosenbusch, P. Lemonde, G. Santarelli, P. Wolf, A. Clairon, A. Luiten, M. Tobar, C. Salomon, *J. Phys. B* **38**, 449 (2005)
21. G. Wilpers, T. Binnewies, C. Degenhardt, U. Sterr, J. Helmcke, F. Riehle, *Phys. Rev. Lett.* **89**, 230801 (2002)
22. T.E. Mehlstäubler, J. Keupp, A. Douillet, N. Rehbein, E.M. Rasel, W. Ertmer, *J. Opt. B* **5**, 183 (2003)
23. R.J. Rafac, B.C. Young, J.A. Beall, W.M. Itano, D.J. Wineland, J.C. Bergquist, *Phys. Rev. Lett.* **85**, 24622465 (2000)
24. J. Dick, in *Proc. 19th Annual PTTI Systems and Applications Mtg*, 133 (1987)
25. J. Dick, J.D. Prestage, C.A. Greenhall, L. Maleki, in *Proc. 22nd Annual PTTI Systems and Applications Mtg*, 487 (1990)
26. G. Santarelli, C. Audoin, A. Makdissi, P. Laurent, G.J. Dick, A. Clairon, *IEEE Trans. Ultrason. Ferroelectr. Freq. Control* **45**, 887 (1998)
27. J. Gao, *OSA Trends in Optics and Photonics (TOPS) 73, Conference on Lasers and Electro-Optics*, OSA Technical Digest, Postconference Edition (Optical Society of America, Washington DC, 2002), Vol. 175
28. A. Quessada, R.P. Kovacich, I. Courtillot, A. Clairon, G. Santarelli, P. Lemonde, *J. Opt. B: Quant. Semiclass. Opt.* **5**, 150 (2003)
29. M. Notcutt, L.-S. Ma, J. Ye, J.L. Hall, *Opt. Lett.* **30**, 1815 (2005)